

Remote Sensing-based Morphometry on the Petroliferous Cambay Rift Basin (Gujarat, Western India)

Surabhi K¹, Mery Biswas² and Soumyajit Mukherjee^{3*}

¹Department of Civil Engineering, Manipal Institute of Technology, Manipal - 576 104, India

²Department of Geography, Presidency University, 86/1, College Street, Kolkata - 700 073, India

³Department of Earth Sciences, Indian Institute of Technology Bombay, Powai, Mumbai - 400 076, India

*E-mail: soumyajitm@gmail.com, smukherjee@iitb.ac.in

Received: 18 June 2023 / Revised form Accepted: 19 September 2023

© 2024 Geological Society of India, Bengaluru, India

ABSTRACT

The Cambay Rift Basin (CRB) is a product of rifting in western India that formed during India's drift following the breakup of Gondwanaland during the Early Jurassic and Tertiary Periods. Being petroliferous, the basin has attained paramount attention. Seismicity in CRB proves its present-day tectonic sensitivity. Several NNW-SSE, NW-SE and NE-SW trending faults regulate the channel morphology within a portion of the basin. Drainage network systems are proxies of active faulting. Geomorphic indices e.g., long profile analysis, basin-scale parameters, stream length gradient index and sinuosity index along the main channels in the five watersheds have been evaluated in this work. The Index of Active Tectonics (IAT) is derived from the basin-scale parameters and is clubbed into three classes: class 1 (IAT = 1.4 - 1.9), class 2 (IAT = 1.91 - 2.4) and class 3 (IAT = 2.41 - 2.9). IAT Class 1 indicates a higher present-day tectonic activity than the other watersheds such as 1, 2 and 5. Watersheds in the northern and eastern Cambay region (watersheds 3 and 4, and portions of 1 and 5) exhibit higher tectonic activity. Slope breaks and low sinuosity index near the crossing-points in these northern and eastern portions indicate active / weak zones. Along these zones, channels incise vertically and more efficiently than laterally in watersheds 3 and 4. These weak zones may indicate older structures such as lineaments and faults. The Ahmedabad-Mehsana block in watershed 3 and partly in watershed 1 within the CRB with several oil fields are tectonically highly active. Therefore, well-bore stability studies need to be carried out in this block.

Keywords: Morphometry; active tectonics; geodynamics; petroleum geology; structural geology

INTRODUCTION

Petroliferous tectonic rift basins are crucial to study for their tectonics, structural geology and morphotectonics (e.g., Dwivedi, 2016; Dasgupta and Mukherjee, 2017, 2019). The rift basins are characterized by faulted margins and interiors, asymmetric geometry in vertical cross-sections and rift fill sediments with varying thickness, etc. Such basins' tectonic analyses can reveal mechanisms for uplift, incision and sediment depositional pattern (Withjack, 2002).

Cambay Rift Basin (CRB) developed as the Indian plate migrated northward following the separation from Gondwanaland in the Early Cretaceous (Biswas, 1982, 1987; Danda et al., 2017). It is an elongated

intra/peri-cratonic basin and/or a marginal aulacogen located in Gujarat. CRB cumulatively occupy ~ 59,000 km². Recently Chouhan et al. (2023) presented an evolutionary model of the CRB based on their gravity studies. These authors interpreted the presence of a magmatic underplating layer from mid-crustal depth from the central part of the CRB. Nagarjuna et al. (2023) deciphered based on magnetotelluric methods a spatially heterogeneous lithosphere from the CRB.

The Indian petroliferous basins are divided into four categories in terms of current and potential hydrocarbon exploration (Biswas, 2012; Hafiz, 2019; Phaye et al., 2021). CRB comes under the Category I basin: as per the Directorate General of Hydrocarbon (DGH, India): a proven reservoir (Biswas, 2012). Tertiary and Quaternary sediments in the CRB e.g., sandstones and shales store commercially producible hydrocarbon (Gupta et al., 2012). The basin is one of the most prospective Indian oil-producing fields (Biswas, 1987).

CRB is bordered by the Precambrian Aravalli rocks in the NE and discontinuous faults and Deccan traps (eruption in 67-68 Ma; Mukherjee et al., 2017) in the SW and the SE (Repository Fig. 1A). Repository Fig. 1C presents the plate velocities in the International Terrestrial Reference Frame (ITRF) 2008 (blue dash arrow) and the Indian Reference Frame (red solid arrow) in the northern CRB. The residual motion deformation rate has been estimated to be 1 to 1.8 ± 0.1 mm yr⁻¹ at SE part of the CRB (Mahesh et al., 2012) (Repository Figs. 1B, C). Repository Fig. 1D presents the stratigraphy of the basin. The basin is delimited at north by hilly regions of SE Rajasthan, and at south by alluvial terrain of Gujarat (Maurya, 1995; Merh, 1995).

In the basinal region, several geomorphic anomalies have been identified (Babu, 1977). Some of the rivers in the CRB modified their courses. Climatic and/or tectonic changes could be the reason (Babu, 1977). Faults in the CRB regulate the morphology of the valley floor of the basin. In other words, the morphologic changes in the river system are induced by the successive reactivation of these faults.

There are three main Precambrian trends in and around the CRB. These are Dharwar trend (NNW-SSE), Aravalli-Delhi trend (NE-SW) and Satpura trend (ENE-WSW) (e.g., Biswas, 1982; Kundu and Wani, 1992). These trends affected the present-day structure of the CRB. Interaction between NNW-SSE and ENE-WSW trends, represented by various faults and lineaments, controls the structural framework of the basin (Mathur et al., 1968; Wani and Kundu, 1995; Das and Solanki, 2020). These two sets of trends have also been prevalent in the northern part of the western continental margin of India (WCMI) (Mukherjee et al., 2020). Intercontinental rifting produced the former, whereas

intra plate pericratonic rifting developed the later (Choudhury et al., 2019).

Drainage morphology and morphotectonic indicators disclose the Quaternary tectonics (Argyriou, 2016; Singh, 2014, 2015; Prakash, 2017). Landform genesis and evolution by active tectonics can provide fundamental information needed to constrain long-term deformation and tectonics (Verrios, 2004; Bahrami, 2012; Sukristiyanti et al., 2018; Dubey and Shankar, 2020). Recently, various workers morphotectonically analyzed watersheds (e.g., Singh, 2014; Pande and Moharir, 2017; Prakash, 2017; Adhikary et al., 2018; Baruah et al., 2020; Biswas et al., 2022). Several studies have demonstrated the usefulness of erosional landscapes for detecting tectonic signatures over time scales of 10^3 – 10^5 years. A number of key studies calculate the relationships between uplift rates and erosional landscapes, with a focus on bedrock river profiles (Hack, 1957, 1973; Kirby and Whipple et al., 2013; Chen, 2015; Gentana et al., 2018). These models have revolutionized geomorphic methods (Prakash, 2017; Kumari et al., 2021).

Although CRB has been the subject of numerous geoscientific researches, its morphometric analysis in the context of active tectonics remained a due. The present study applies morphotectonic indicators to assess the active tectonics of CRB in watershed-scale. We used Analytical Hierarchical Process (AHP) to achieve more appropriate ranking of tectonics. Several criteria are applied to determine the tectonic influence on the rivers. The weight was determined using AHP. Satty (1977) introduced the multi-criteria decision-making process using the AHP. Despite few geomorphic works (e.g., Pancholi et al., 2017), none has studied morphometric indices in conjunction with the AHP technique to pinpoint patterns of relative tectonic activity in the CRB. Recently Desai et al. (2023) studied the geomorphology of the Lower Sabarmati river basin. The work commented on the paleoenvironmental changes of the terrain only, and not about the neotectonics effects.

The mature oil field such as Ankalweshar in CRB has been counted as a potential region for carbon sequestration (Ganguli, 2017). In such a scenario as well as for well-bore stability-related studies generally relevant for all oil fields, knowing recent day tectonics is essential (e.g., Salarian et al., 2012).

TECTONIC EVOLUTION OF CRB

CRB's tectonics is significantly connected with the origin and evolution of the Indian plate. CRB is NNW-SSE elongated formed during the Mesozoic and subsided more rapidly during the Tertiary (Biswas, 1987; Biswas, 1999).

The basin comprises of three major structures: rift-induced extensional faults, transfer zones and asymmetric half-grabens. During rifting, two types of extensional faults were produced: N-S to NNW-SSE trending listric normal faults and NE-SW to ENE-WSW transfer faults following the Dharwar and Aravalli–Delhi trends (Kundu and Wani, 1992; Clark et al., 1995, 2004). Transverse E-W to ENE-WSW faults divide the CRB into several blocks from north to south (Repository Fig. 1B). Few of these faults are old and reach the basement (Gupta, 1981; Kaila et al., 1990).

Previous workers divided CRB into five blocks. Towards south these are- Sanchor-Patan, Ahmedabad–Mehsana, Cambay–Tarapur, Broach and Narmada blocks (Mathur, 1968; Repository Fig. 1B). The basement faults control tectonics of these blocks. Alternately, CRB can be divided based on geomorphology into three primary zones: the upland zone, the pediment zone and the alluvial zone (Raj, 2012). Precambrian Aravalli rocks constitute the upland region, located in the NE part of the study region. The Aravalli range shaded sediments mostly in the Cambay basin (Babu, 1977; Sahoo and Choudhuri, 2011; Mohan et al., 2019). The upland regions of NE section of the watershed 3 and 4 are highest in elevation - between 300 to 600 m above the sea

level. Southwest of the upland zone is the pediment zone that slopes SW to SSW. The elevation of this area ranges from 150 to 300 m above the mean sea level before gradually decreasing to 75 m where it merges with the alluvial plain. The alluvial zone is located southwest of the pediment zone, with 25-75 m elevations above the mean sea level (Raj, 2012).

The study area consists primarily of Quaternary alluvial sediments surfaces covering CRB with a minor portion of the Precambrian upland region at NE section outside CRB. In order to look at the entire watersheds 2, 3 and 4, it was necessary to include some portions outside CRB.

Seismicity in and around CRB

Gujarat is one of the world's most seismically active intraplate zones. The studied region consists of five watersheds, which are seismo-tectonic in nature (Fig. 1A). The seismic zoning map of India places CRB within zones III and IV (BIS, 2002). The expected magnitudes of maximum credible earthquakes (MCEs) in zones III and IV are 6.0 and 7.0, respectively. Two notable historical earthquakes occurred in 1848 (Mw 5.7) and 1969 (Mw 5.5) in the northern CRB (watershed 5) (Rastogi et al., 2013). Following the 2001 Bhuj earthquake, it is now possible to monitor seismicity at the micro-scale in Gujarat and the surrounding areas. The Institute of Seismological Research's (ISR, at Gandhinagar, Gujarat) seismic network has been operational since 2006 (Fig. 1A1). As per a review of data for the last 10 years from BIS (2002) and Rastogi (2013), the northern section of CRB has seen an increase in seismic activity due to stress perturbation (Pancholi et al., 2022), with several minor earthquakes reported in this area. In 2010 and 2017, two earthquakes of Mw 4.2 and 4.1, respectively, occurred in CRB. In addition, 29 earthquakes with magnitudes ranging 3-4 Mw have been registered in this region since 2007.

Since 2007, the Sanchor-Patan block (watershed 4 and partly 5) has experienced > 20 earthquakes with 3-4 magnitudes. Between mid-2006 and 2014, the Gujarat State Seismic network reported ~ 625 earthquakes with magnitudes ranging from 1 to 4.4 in CRB. As per the recent seismicity patterns, the central part of the basin near Mehsana (part of watershed 5) tend to be comparatively less active (Pancholi, 2017). From all the data it is clear that the south-western part of CRB (parts of watersheds 2 and 5) is seismically less active while the northern portion (watershed 1 and part of watershed 5) is active influencing the tectonics of the area. Figures 1B, C are the interpolation of magnitude and depth (m) of nine earthquakes. The magnitude and depth are positively correlated (Fig. 1B1). The magnitude of earthquake is generally higher inside CRB and less at the NE and the SE portions. The Cambay area has greater depths (~ 35 m) of hypocenter of earthquakes (<https://earthquake.usgs.gov/earthquakes/search/>, accessed on 03-April-2022). Slope direction in figures 1C-C1 reveals that the hypocenter depth increases towards CRB.

METHODOLOGY

Shuttle Radar Topography Mission (SRTM) - Digital Elevation Model (DEM) data sets were used from the United States Geological Survey (USGS) Earth Explorer. We used six tiles of SRTM DEM (2005) with a 3 arc second resolution. In the platform of QGIS 3.14, five watersheds were extracted following the rules of fill DEM to flow accumulation. Watersheds were delineated using stream feature class tools. Geometric features (e.g., area, basin perimeter and basin length) were retrieved and measured automatically in QGIS.

For the morphotectonic analysis of CRB, both linear and aerial amplitudes were obtained to evaluate active tectonics in the watershed-scale dimension. The thalweg long profiles of rivers reflect the results of the past and the present geomorphic processes in the basin. The

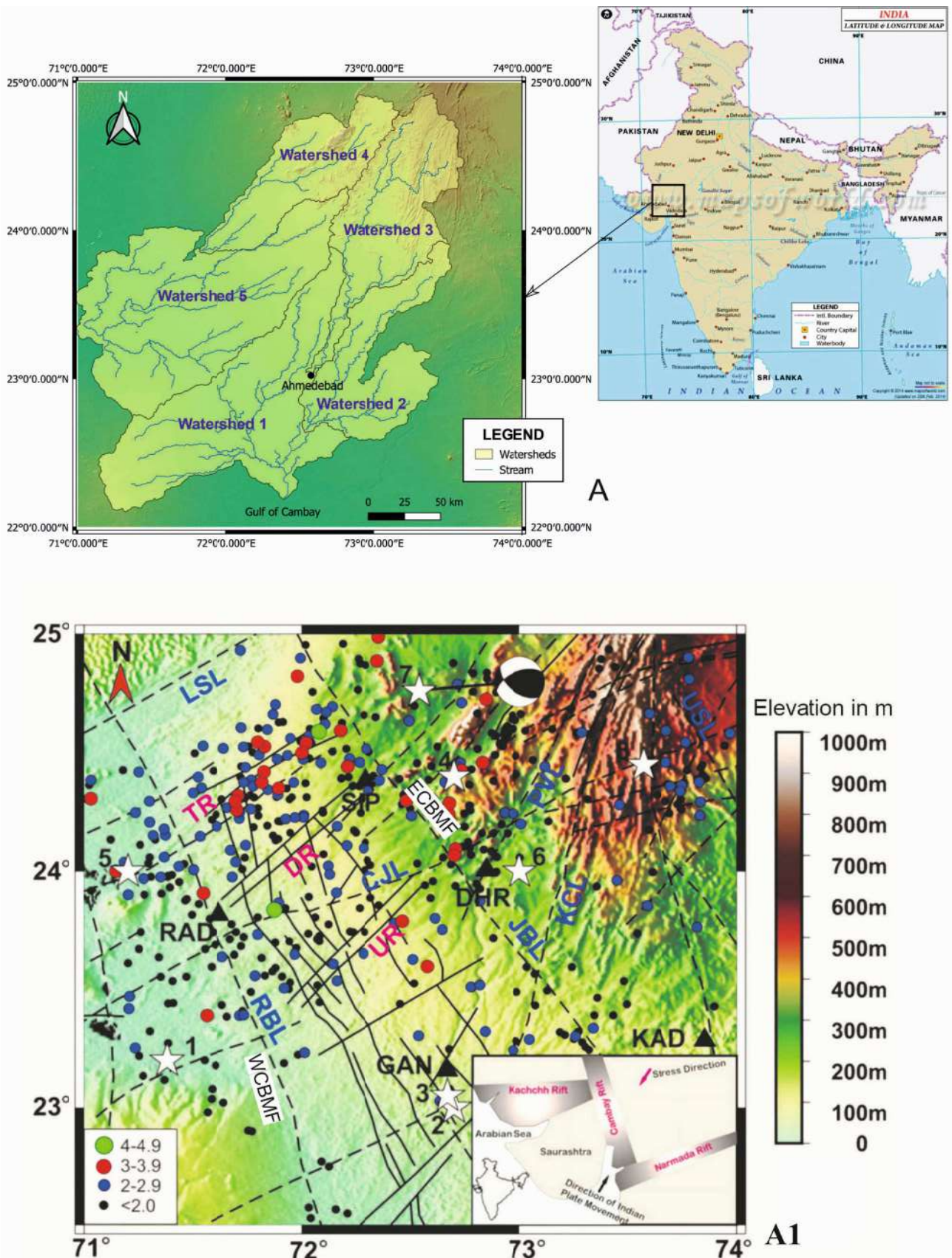


Fig. 1. A- Map showing the study area (22°N-25°N and 71°E-74°E). Left: Watersheds extracted from DEM in QGIS overlaid over the hillshade map. Right: Map of India where the study area is marked by a black rectangle. **A1.** Seismic events in CRB and its surrounding (Choudhury et al., 2019). See Chouhan et al. (2020) for sub-surface structures in the watersheds. *Abbreviations:* CJL: Chambal–Jamnagar lineament, DR: Diyodar ridge, ECBMF: East Cambay Basin Margin Fault, JBL: Jaisalmer–Barwani Lineament, KCL: Kishangarh–Chipri Lineament, LSL: Luni–Sukri lineament, PVL: Pisangan–Vaditagan Lineament, RBL: Radhanpur–Barmer Lineament, TR: Tharad ridge, UR: Unhawa ridge, USL: Udaipur–Sardarpur Lineament, WCBMF: West Cambay Basin Margin Fault; DHR: Dharoi. GAN: Gandhinaga,; KAD: Kadana, RAD: Radhanpur, SIP: Sipu. Locations 1, 2 etc. are the places of seismic data.

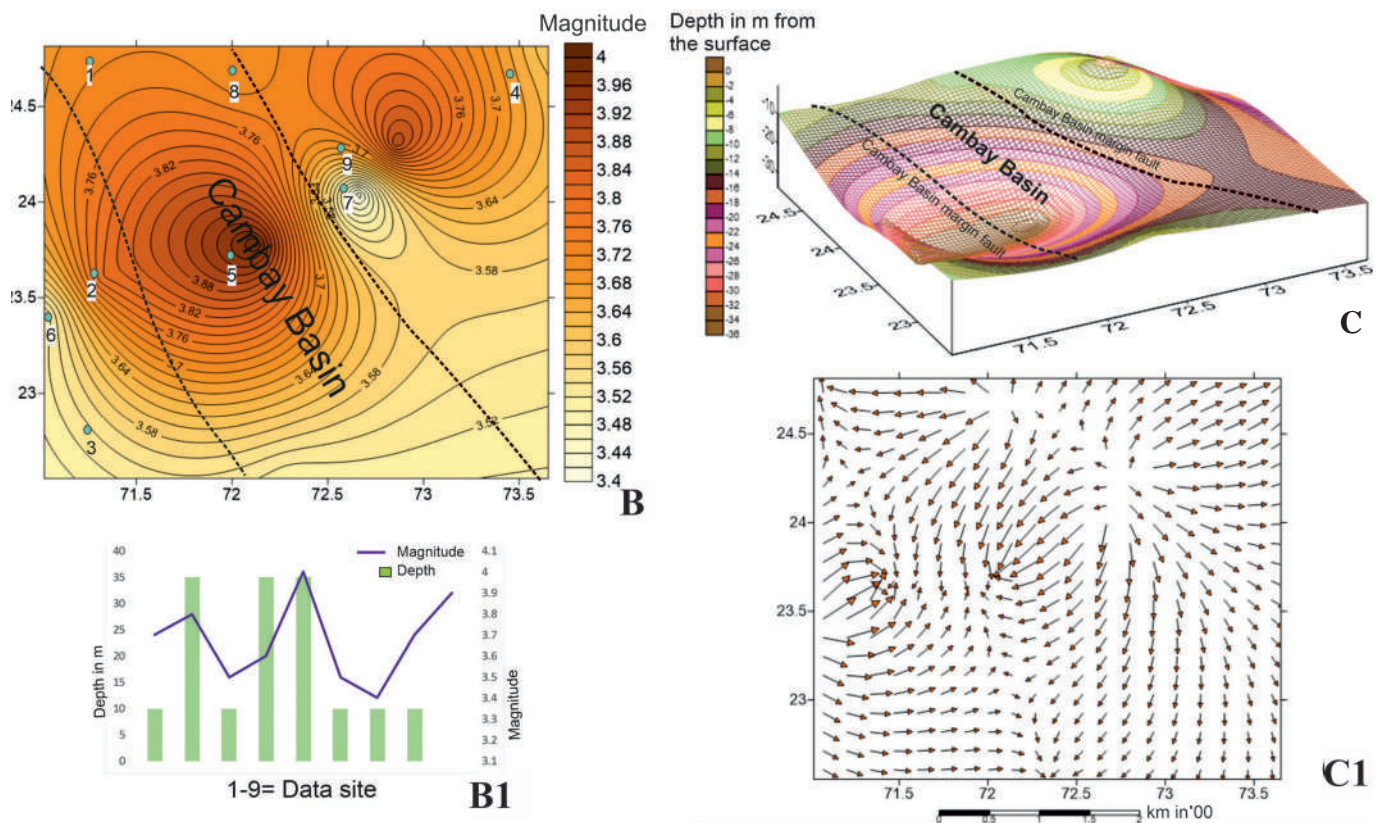


Fig.1B. Isolines of earthquake magnitude over the study area covering the Cambay basin. **B1.** Graphical representation of earthquake magnitude and depth where the bars represent the depth and the line is magnitude. **C.** Representation of earthquake depth (m) data. Cambay basin margin faults are marked. **C1.** Slope of the earthquake magnitude trend that increases towards Cambay basin area.

correlation coefficient (R^2) displays the fitting suitability of exponential curves representing the probable active channel. The stream length gradient index (SL) for channel slope explains how the gradient changes over the stream-length of the chosen channel segment. Sinuosity index (SI) connotes the erosional properties- aggradation and degradation of sediments in a river long profile. The knickpoints are then identified by plotting the faults and lineaments over the main channels for each watershed. The intercepting points are marked over the long profiles as well as in the Google Earth Pro (7.1, 2015). After that, the SI for each segment was calculated (Raˆdoane et al., 2003; Khalid and Ashmawy, 2016). This helps to identify potential tectonic locations of a particular area or the local level tectonic sensitivity. SI describes the degree of meandering of a river and constraints the geomorphologic type of the river. It is the measure of deviation of a channel from the shortest possible path between the two points. SI indicates the pattern of channel from which a potential fault zone or lineament can be inferred.

Six basin-scale factors viz., Basin shape Index (B_s), Form Factor (R_f) Hypsometric Integral (HI), Circularity Ratio (R_c), Elongation Ratio (R_e) and Lemniscate Coefficient (k) (Repository Table 1) were employed to calculate the Index of Active Tectonics (IAT) (e.g., Mahmood and Gloaguen, 2012; Kumar et al., 2017; Gupta and Biswas, 2022) for all the watersheds. The results are grouped into three classes for each factor and integrated, and then presented in the form of IAT of the watersheds. IAT values are divided into low, moderate and high. Such a scheme of classification of IAT has been practiced widely in geomorphology (e.g., Anand et al., 2017). The high value for IAT indicates the low tectonic activity in the terrain. Drainage density and the dissection map were also prepared.

AHP technique was used to integrate the individual IAT parameters into this work in order to rank active tectonics more appropriately. AHP's mathematic foundation is built in the eigenvector method (Saaty,

1977; Aram and Arian, 2016). It is a popular method for computing weighting factors using a preference matrix. This matrix expresses the relative preference amongst the factors (B_s , R_f , HI, R_c , R_e and k) by comparing relevant criteria/factors for a selection in a pair-wise approach. As a result, each element must be allocated a number representing its relative significance / preference over the other (Dyer and Forman, 1992; Aram and Arian, 2016). The comparison uses a scale of 1 to 9 to represent the intensity of importance (preference/dominance), and each factor (B_s , R_f , HI, R_c , R_e and k) is compared with the other in terms of their importance (Saaty, 1980; Alipoor et al., 2011). Saaty (1977) proposed a comparison scale with values ranging from 1 to 9 describing the level of significance (preference/dominance). Values of Satty scale rank 2, 4, 6 and 8 are the intermediate values, while 1, 3, 5, 7 and 9 represent equal significance, considerable importance of one element over the another, strong or essential importance, extremely strong importance and extreme importance, respectively (Argyriou, 2017).

By using a free web-based AHP solution and carrying out an appropriate pair-wise comparison of all criteria, the pair wise comparison matrix is created automatically. The Consistency Ratio (CR) was calculated to determine whether the calculated judgement weights of considered parameters (Eigen vector) show sufficient consistency. The comparison matrix can be marked with accurately if the value of C.R is < 0.10 . RI is constant as 1.25. The calculated C.R value is 0.06821 and CI value is 0.0852693. The following formulae were used to calculate the CR (Pant, 2022):

$$CI = [\lambda_{max} - n / (n - 1)] \quad \text{eqn. 1}$$

$$CR = (CI - RI) \quad \text{eqn. 2}$$

Here CI: Consistency Index, RI: Random Consistency Index;

λ_{max} : computed average value of the weight. There is a randomly generated comparison matrix as per the Saaty scale. Particular value is offered for a number of factors (n). The 'n' value is 6 in this study. However, in this case, it is determined automatically using the AHP Priority Calculator. Here the calculated CR is < 0.1 (0.06821). Therefore, the pair-wise matrix has a decent level of consistency (Saaty, 1991; Birjandi et al., 2020).

RESULTS AND DISCUSSIONS

The extracted watersheds cover the areas under Ahmedabad-Mehsana, Cambay-Tarapur and a small part of the Patan-Tharad-Sanchor blocks. All the rivers in the watersheds flow towards ~ SW.

Watersheds 1 and 3 are parts of the Sabarmati river basin that are considered in two parts in this study as per the tributary-based two channel systems. The rivers in watersheds 3 and 4 originate in two distinct parts of the Aravalli hills, around 546 m and 337 m elevations, respectively. They flow across a few major faults and lineaments such as the NNE-SSW trending Pisangan-Vadhanagar Lineament (PVL), the Jaisalmer-Barwani lineament (JBL), the NNE-SSW trending Kishangarh-Chipri Lineament (KCL), the NE-SW trending Chambal-Jamnagar lineament (CJL), Rakhabdev Lineament (RL) and the NW-SE trending Himatnagar Fault (HnF). These lineaments are plotted in figure 4. The path of the master stream of watershed 3 and 4 are further influenced by NNW - SSE trending the Bok Fault (BF) and the East Cambay Basin Margin Fault (ECBMF). Precambrian Dharwar orogenic structures are associated with the NNW - SSE lineaments (Raj, 2012). Major faults that run NE-SW to ENE-WSW separate the CRB into transverse blocks. This indicates that the previously existing NE-SW trending lineaments or faults reactivated during CRB's genesis. The ECBMF in the basin, which runs NNE-SSW (Mathur, 1968; Raju, 1968), has a strong surface expression in aerial photos (Agarwal, 1996). The presence of faults or lineaments alter the rivers' profile. This can deviate the river profiles from their ideal forms (Chen et al., 2006). Rivers in the five watersheds cut across various geologic formations. The flow directions are possibly structurally controlled (watersheds 1-5).

Geomorphic analyses provide vital input in petroleum geosciences studies (e.g., Mitra and Agarwal, 1996). This is because the drainage pattern can be fault or basement structure-controlled. Neotectonic stress regime can work with them and produce the surface morphology (e.g., Mazumder et al., 2012).

Our study from CRB reveals that the Ahmedabad-Mehsana block (watershed 1 and part of watershed 5) with maximum oil fields belong to the region of high and moderate tectonic activity. Most of the fault crossing points (FCP) and lineament crossing points (LCP) are located in watersheds 1, 2 and 3 indicating that those watersheds are tectonically active. Only four FCP and LCP are located in watersheds 4 and 5. Therefore, CRB's future work scope should include well-bore stability issues for the Ahmedabad-Mehsana block.

Spatial Scale Analysis

Relief, aspect and slope differentiation

Results obtained from the geomorphic calculations are correlated with respect of slope and tectonics of the area. Slope is an important element for geomorphic studies. SRTM DEM data were utilized to create maps in the current investigation. The relief map (Repository Fig. 2A) displays the elevation variation with the geomorphic units. The slope map (Repository Fig. 2B) shows that the slope ranges from ~ 0 to ~ 20° in the plains and pediment zone (watershed 1, 5 and part of 2). But in the upland zone (portions of watershed 2, 3 and part of 4) it ranges ~ 20 to ~ 60°, and in the NE part (parts of watershed 3 and 4) it exceeds 60°. Watersheds 1, 2 and 5 consist of gentle slope (< 20°), and watersheds 3 and 4 possess steeper slopes (40 - 60° and

> 60°). Hence, 70% of all the watersheds have low slope (0 - 20°) towards SW. The elevated catchment of the study area (watersheds 3 and 4) has steeper slope than the middle and downstream parts (watersheds 3 and 4). The aspect map indicates the direction the slope facing, which is measured clockwise from N (Repository Figs. 2C-D).

Drainage density (Dd) and dissection index (DI)

Dd is characterized by drainage lines that are specified by slope and topographic ruggedness. Length of drainage lines per km² of area increases with increase in drainage line density. Steeper the slope and denser the faults, greater is the Dd. Repository Fig. 3A presents higher values of Dd (> 0.4) near the confluence zones in watershed 1. In the catchment area of watersheds 2, 3, 4 and 5 several first-order streams are generated. This catchment area is bordered by NNW - SSE elongated CRB along with several lineaments.

DI is the ratio between the relative relief to the drainage density. Its higher values represent the most dissected patches. The lower values indicate that the areas are less dissected by the existing drainage lines due to lower relative relief, gentler slope and lower stream power. The parameter reveals that the elevated NE parts of the study area (watersheds 3 and 4) are highly dissected as the streams are in young stage with prolific energy and steep slope/relief (Repository Fig. 3B).

Geologic setting, soil properties, vegetation and rainfall intensity influence the Dd of the basin. Dd values are higher in drainage basins with impermeable lithology, high relief and terrains with poor infiltration potential (Shukla, 2013).

Drainage pattern

River incision, alteration in basin asymmetries, drainage structure and complexities and river deflections cumulatively define the drainage pattern (Cox, 1994). Erosion and incision are the key aspects of morphotectonic analysis and are strongly associated with the drainage behavior.

Anomalies in drainage, identified as variations from common regional patterns may reveal tectonic deformation (Zernitz, 1932; Howard, 1967). Rectangular pattern of rivers indicates a basement with perpendicular network of lineaments in watersheds 1, 3 and partly 5 (Repository Fig. 3C). Where tributaries join the main river following the slope and the bedrock has no particular structure, erosion promotes in all directions resulting in a dendritic channel pattern. These have been observed in watersheds 1 and 5 (Repository Fig. 3C).

Linear-scale geomorphic indices

The mechanical and the physical characteristics of the sediments are two of the important controlling factors governing the geomorphic indices. The indices used in this analysis indicate active tectonics as follows:

Long profile analysis

Long profile of a river is a graph of river bed elevation vs. distance along the thalweg of the channel. The profile is a product of the past and the present geomorphic processes of the basin. These profiles are influenced by tectonics, lithology, fluvial incision and base-level adjustment (Larue, 2008). Such profiles can reflect the evolution of the watershed as well as its geologic structure and sediment dynamics (Leopold and Maddock, 1953; Costigan et al., 2014).

In this study, source to mouth plots were used for the longitudinal profiles for the five watersheds. These profiles across the hilly ranges attain smooth concave-up geometries indicating prevailing channel incision mechanism. The exponential curve fit and the computed Y_c (the calculated or estimated value of dependent variable) values with variance of coefficient as R^2 imply the degrees of tectonic activeness

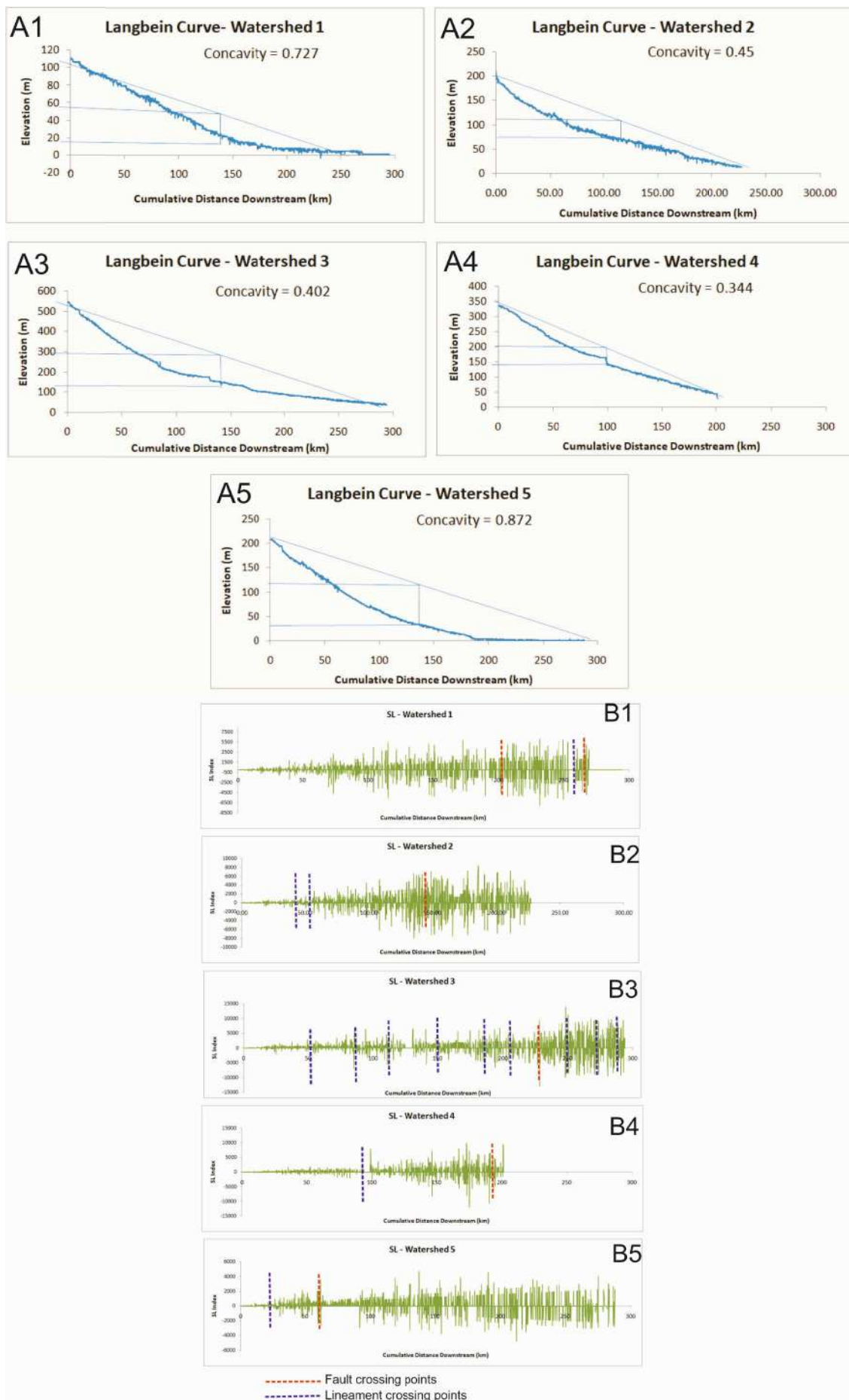


Fig. 2A. Langbein curve for each watershed with their respective concavity index values. **B.** SL Indexes (variation along long profile) for each watershed indicate the changes of stream length variation with gradient

of the basins. Slope breaks as knickpoints signify regional uplift and incision. The highest R^2 values in exponential curve fit for the watersheds 2, 3 and 4 indicate that the channels are active and they are closer to class 1 or 2 in the IAT value ranges. The high magnitudes indicate that the watersheds have been experiencing high to moderate tectonic activity. Both the watersheds 1 and 5 have the greatest R^2 values in a logarithmic curve fit, indicating ongoing moderate tectonic activity and they fall under the IAT's classes 2 and 3, respectively (moderate to low active group). Remarkably, watershed 3 possesses two slope breaks with knickpoints revealing tectonic uplift and rejuvenation.

Concavity Index (CI)

When the steady-state condition (rate of uplift = rate of erosion) is reached, longitudinal profiles of bedrock rivers generally have a concave-up form (Sobel et al., 2003; Wobus et al., 2006). The concavity of the river longitudinal profile is determined by factors viz., climate, base level change and tectonics (Zaprowski, 2005; Sinha and Parker, 1996). Channel concavity can be estimated by different methods. Several authors used a δ -index as its measure. Instead, the Langbein concavity index (Larue, 2011), was calculated in this work. To compare the concavities, Langbein curves are plotted for the five watersheds (Figs. 2A1-A4). The surficial processes by exogenetic agents have shaped the watersheds and the consequent streams reflect its erodibility range resulting the concavity (Bierman and Montgomery, 2014). If the concavity value is near zero, the profile is linear. For concavity index $H \sim 1$, the profile is L-shaped. In general, the longitudinal profiles of equilibrium streams are upwardly concave (Strahler, 1952), but lower CI (< 0.3) indicates steep headwater and debris flow, medium CI (0.3-0.7) imply fluvial incision-dominated streams, and high CI (> 0.7) connotes alluvial rivers (Bierman and Montgomery, 2014).

Lower concavity values indicate higher tectonic sensitivity. The calculated CI values are 0.72 (watershed 1), 0.45 (watershed 2), 0.40 (watershed 3), 0.34 (watershed 4) and 0.87 (watershed 5), respectively. Watershed 4 shows the lowest CI followed by watershed 3.

Stream-length gradient index (SL)

As per Keller and Pinter (2002), SL is defined by the alteration in channel slope, that can arise due to disparity in bed-rocks' strengths and active tectonics of the area. The change in the river profile might be caused by the lithologic, tectonic or environmental elements (Hack, 1973; Bull, 2007; Elias, 2015). SL index is a powerful tool for identifying anomalous variations in the river. The most likely causes of SL changes include variations in erosion tolerance to outcropping lithologic units, subsurface processes such as active faulting and slope failure.

SL index is used to estimate the relative strength of active tectonics. The index detects recent tectonic activity based on its unusually high values on certain rock types. For example, high SL indices on an area having soft rocks such as shale can suggest recent tectonic activity. Higher SL values, on the other hand, can indicate that the streams cross (strike-slip) faults (Keller and Pinter, 2002). Tectonic behavior can also be indicated by an unusually low SL.

SL values for more than 1000 points were obtained from the five watersheds along the long profiles. Graphs (Figs. 2B1-5) were prepared using these results and the average SL index for each watershed was obtained, which depicts different degrees of tectonic activeness. The average SL values of watersheds 1 to 5 are 32.89, 71.98, 176.78, 132.81 and 59.03, respectively. Lower SL values such as 32.89 and 71.98 (in watersheds 1 and 2, respectively) indicate the existence of lineaments. Higher values in watersheds 3 and 4 (176.78 and 132.81, respectively) indicate an influence of the major lineaments crossing points viz., Kishangarh-Chipri Lineament (KCL), Chambal-Jamnagar Lineament

(CJL), Pisangan-Vadhanagar Lineament (PVL) and Jaisalmer-Barwani lineament (JBL). This was the case with watersheds 3 and 4. Watershed 3 has a high SL value. This indicates recent tectonic activity in the watershed. This further suggests that the master streams are flowing along the lineaments.

Micro-scale study of lineament/fault crossing points and SI

Knickpoints are the relief breakpoints along drainage thalweg profiles. The formation of knickpoints are the major geomorphic expressions of fault offset in bedrock rivers (Naccio, 2013). Faults and lineaments have been plotted along with the master streams of each watershed. It is distinctly observed that all the drainage lines crossing CRB in watersheds 1, 3 and 4 are straight. This indicates vertical incision. The drainage lines are mostly parallel to the basement faults and are transverse to the hitherto unnamed listric normal faults referred by Mazumder et al. (2012) (Repository Fig. 4A).

The geomorphic significance is assessed in micro-scale study where potential knickpoint sites are marked and incorporated by mapping faults and lineaments along and across the consequent channel of each watershed. The superimposed faults and lineaments denote few crossing points where SI changes across those points due to erosion / incision. The points of intersection between channels and faults / lineaments indicate the tectonic disturbances with the formation of possible knickpoints where rejuvenation occurred. The rivers intersect lineaments and faults and have been denoted by points (Repository Fig. 4B). Repository Fig. 4C presents the regional geologic formation of CRB and its adjacent area along with the regional structures – Delhi trend, Aravalli trend and Satpura trend. The LPC1A, LCP1B, FCP1A and FCP1B are marked along all the master streams (Repository Figs. 3A1, 5 A1-4, B1- 3; 6A1-3, B1- B3). These points can assess the channel straightness of the particular stretch of the river. Drainages follow these trends. The CBR boundary is transverse to those trends and such structural complexity induce the channel morphologic anomalies.

These LCP and FCP points are marked in longitudinal profiles of the consequent channel of each watershed. Slope break is noticed near the LCP and FCP along the longitudinal profile of each watershed (1-5). Repository Figs. 5A1 and B1 present the longitudinal profiles of watersheds 1 and 2 along with the intersecting points. In Repository Figs. 5A2 - A4, three segments are marked. Calculated SI values of 1.04 and 1.08, for watershed 1 and 2, respectively determine the straight channel and a magnitude of 1.19 indicates sinuous course in watershed 1. These three segments are named as FCP2A-FCP1B, LCP1A-LCP1B and LCP1B-FCP1, respectively (Repository Fig. 5A5). Similarly, Repository Fig. 5B1 shows the river long profile of watershed 2 where two lineament crossing points and one fault crossing point and Figs. 5B2 - B3 show Google Earth imagery with four segments with calculated SI values for all watersheds. Results show prominent anomalies e.g., straight (SI = 1), meander (SI = 1.9), sinuous (SI = 1.1) and again straight (SI = 0.98) downstream (watershed 2) (Repository Fig. 5B4). The calculated SI differs from the segments before and after the crossing LCP and FCP points due to the tectonic response (watershed 2).

The watershed 3 (Fig. 3A1) contains most rugged topography and is drained by the longest channel. It consists of nine intersecting points. One of them is FCP, while the others are LCP. Considering such points on the river profile, 11 segments were marked to evaluate the SI anomalies (Fig. 3A2) with respect of tectonic interference. SI for each small segment was obtained and the results disclose an alternate nature of straight and sinuous course. Remarkably a single meandering pattern (SI = 2.2) was observed between LCP5 and LCP6 and it again turns to sinuous (SI = 1.2) downstream. The low SI values indicate weak zones or presence of lineaments / faults with more vertical incision.

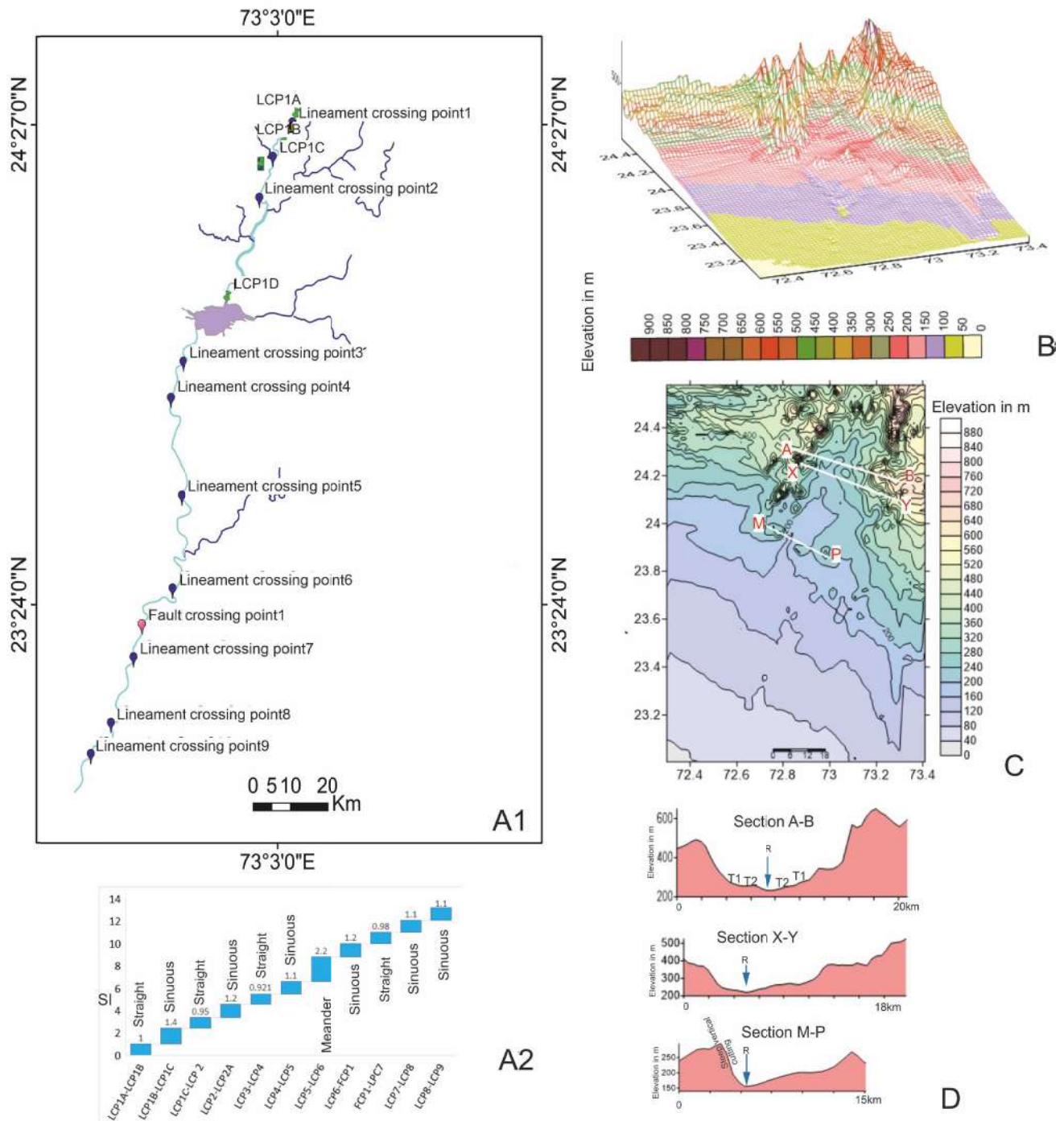


Fig. 3. A1. Location of nine lineament crossing points and one fault crossing point of the main stream of watershed 3. **A2.** Continuous straight pattern of the channel from the source and in the middle part near LCP4-LCP5 is sinuous and LCP5-LCP6 meander. Again, the rejuvenation executed the channel to be more incised vertically forming alternative straight –straight pattern. **B.** 3D elevation mesh presentation of part of watershed 3 area where the main channel has dissected the valley. **C.** Contour pattern of the area depicting the elevated patches in NE corner. **D.** Layout of three cross sections of the channel as A-B, X-Y, and M-P. Section A-B display the two-river terrace system as T1 and T2, which in downstream as wide valley, but in section M-P steep right-hand side cutting of the channel indicates the presence of LCP2.

3D presentations for watershed 3 (Figs. 3B, C) denote the elevation difference downstream along with contours. Three topographic cross-sections A-B, X-Y and M-P are presented in figure 3D. In A-B section, two prominent river terraces were identified that significantly carry the evidence of tectonic activeness and rejuvenation along the channel. The valley widens downstream along the section X-Y (watershed 3). However, in section M-P, near-vertical cutting in the left bank is noted due to unequal vertical erosion rate (Fig. 3D).

Tectonically active watershed 4 has two crossing points- LCP1 and FCP1 (Repository Fig. 6A1). SI was calculated in four segments

along the channel downstream (Repository Figs. 6A2, A3). All the channel segments of the watershed 4 are tectonically active, as the channel is straight (Repository Fig. 6A4). Presence of faults and lineaments clearly carry the imprint of tectonics of the region in watershed 5. The FCP1 and LCP1 for this watershed in Repository Fig. 6B1 are located in the upstream part of the longitudinal profile (Repository Fig. 6B1). Therefore, four segments are considered along the river to regulate the SI values (Repository Figs. 6B2, B3). In segment 3 (watershed 5), channel pattern changes from sinuous (SI = 1.4) to straight (SI = 1.03) and in segment 4 again it becomes sinuous

(SI = 1.3). This indicates tectonic disturbances. Active tectonics in terms of existing faults /lineaments have controlled the riverine incision and the channel geometry (Repository Fig. 6B4).

Basin-scale Geomorphic Indices

The parameters used to deduce IAT are basin shape index (B_s), hypsometric integral (HI), form ratio or form factor (R_f), elongation ratio (R_e), circularity ratio (R_c) and lemniscate coefficient (k).

Basin shape index (B_s): It is another criterion to distinguish relatively young drainage basins in tectonically active regions. It is the ratio between the lengths to width of a basin measured at its widest point. The intensity of active tectonics may be reflected in the magnitude of B_s . Young basins are elongated around topographic slopes or active faults that are still young. The elongated basins become circular with time (Bull and McFadden, 1977; Saber et al., 2020). The higher the B_s , more tectonically active is the basin. This is indicated by the elongated nature of the basin. B_s is calculated using the DEM and categorized into three classes: class 1 ($B_s > 2.6$); class 2 ($B_s = 2-2.6$) and class 3 ($B_s < 2$). Watersheds 3 and 4 show high values for B_s , hence they are presumably elongated and more tectonically active than the other watersheds.

Hypsometric Integral (HI): The HI is estimated using the minimum, maximum and mean elevation of each watershed obtained from the DEM. This parameter is influenced by rock strength and other variables. An HI value of ≥ 0.30 indicates tectonically unstable basin. High HI values usually indicate that the uplands have not been eroded much, implying a recent landform presumably formed by active tectonics. A recent incision through a young geomorphic landscape may also result in high HI . The HI values were categorized into three classes: class 1 ($HI \geq 0.4$), class 2 ($HI = 0.3-0.4$), and class 3 ($HI = 0.3$). Watershed 4 comes under class 1 having a high HI , which indicates its tectonic instability.

Form Factor (R_f): It is the proportion of watershed area (A) to watershed length squared (L^2). Lower R_f values imply elongated basins, suggesting the basin to be tectonically active. $R_f \sim 0$ indicates a tectonically active basin and ~ 1 connotes a tectonically inactive basin. R_f value ranges are categorized into three classes: class 1 (< 0.2), class 2 ($0.2 - 0.3$) and class 3 (> 0.3). Watershed 3 has a lower R_f suggesting it to be more tectonically active than the other watersheds.

Elongation ratio (R_e): It is the ratio of the diameter of a circle of the same area of the basin to the maximum basin length. This ratio aids to understand the shape of watersheds. In tectonically active environments, drainage basins are more elongated without much uplift. Such basins tend to become more circular (Bull and McFadden, 1977). In general, elongation ratio values are divided into two groups: low value- indicating an elongated watershed, and high value- a circular watershed. Several categorizations of R_e have been used by the previous workers. The four classes of R_e are < 0.7 elongated, $0.8-0.7$ less elongated, $0.9-0.8$ oval, and > 0.9 circular (Schumm, 1956). In this study, all the R_e values for the different watersheds are < 0.7 , so the watersheds are grouped into three classes: Class 1 ($R_e < 0.5$): highly elongated, class 2 ($R_e = 0.5-0.6$): moderately elongated, and class 3 ($R_e > 0.6$): less elongated basins. Since watershed 3 is highly elongated, it is tectonically active.

Circularity ratio (R_c): The ratio between the area of a watershed and the area of a circle with the same perimeter as the watershed is known as the circularity ratio (R_c). Structural disturbances influence R_c . The young, mature, and old phases of the life cycle of the tributary within the watershed are indicated by low, moderate and high R_c values,

respectively. A low value connects structural disturbances, whereas a high value indicates that the watershed is under structural influence. The calculated values of R_c are classified as: class 1 ($R_c > 0.20$), class 2 ($R_c = 0.15-0.20$), and class 3 ($R_c < 0.15$). Watershed 4 comes under class 1 with a higher value of R_c indicating noticeable structural disturbance.

Lemniscate Coefficient (k): Chorley (1957) discussed this parameter to assess the slope of the watershed. It is the ratio of square of basin length to basin area. A high ' k ' value denotes a tectonically active basin. As per this parameter, the basin can be categorized as: class 1 ($k = 4-5$), class 2 ($k = 3-4$) and class 3 ($k = 2-3$). Watershed 3 comes under class 1 having a high ' k ' value (4.19) indicating a tectonically active basin while watershed 5 has a low k value (2.35) indicating it is tectonically inactive (Repository Fig. 7A-F).

Magnitudes for morphometric parameters are presented in the Repository Table 2A for all the five watersheds. All the basin-scale parameters were classified into three classes (Repository Table 2B). Class 1 value shows a tectonically active region (watersheds 3 and 4).

Index of Active Tectonics (IAT)

The result of AHP calculation reveals that the six parameters (B_s , R_f , HI , R_c , R_e and k) are ranked properly for the IAT. A CI value of 0.0852693 and a CR = 0.06821 indicate the satisfactory level of significance.

IAT for each watershed was estimated (Repository Table 3) and the magnitudes were applied in comprehending the evolution of tectonic activity of the CRB. The values of IAT were categorized into three classes in this work: class 1 (IAT = 1.4-1.9), class 2 (IAT = 1.91-2.4) and class 3 (IAT = 2.41-2.9). The low IAT (class 1) indicates a significantly high tectonically active region. Watersheds 3 (IAT=1.5) and 4 (IAT=1.5) come under this class. Watersheds 1 (IAT = 2.1) and 2 (IAT = 2) come under the moderate range of IAT, while watershed 5 (IAT = 2.8) shows a high value implying a less active region.

Hence, the NE part of the study area is tectonically more active than southern alluvial plains. According to Pancholi et al. (2017), Cambay basin's (parts of watersheds 1, 3, 4 and 5) intra-basin faults probably impacted the region's high tectonic activity and reactivated very old geologic features including the NW- JBL, PVL, KCL, CJL and HNF.

Since the Archean Aravalli rocks mainly occur in the NE part of CRB (watersheds 3 and 4), and rivers follow the lineaments of the Delhi-Aravalli system, the watersheds present there have a distinct tectonic imprint. The existing seismic literature of CRB also implies a recent rise in the occurrences of small earthquakes within the northern part of the basin (part of watersheds 4 and 5). CRB has a comparatively inactive southern part (portions of watershed 1). Repository Fig. 7G shows the spatial distribution of the final IAT classes.

Figure 4 is the superposition of IAT map on the geologic map of the study area. IAT values show high tectonic activity along the major lineaments and faults present in the northern part of the CRB (watersheds 3 and 4). From figure 4, it can be understood that portions of watersheds 2 and 5 are the areas with least tectonic activity. The combined results of geomorphic indices (Repository Table 4) and the linear aspects e.g., drainage pattern and SI indicate that the watershed 3 is definitely active. Both watersheds 3 and 4 are located in the northeast part of the study area, where the rivers originated from the Aravalli hills. These rivers flowing from the Aravalli up to the Gulf of Cambay/Khambhat (GOC) cross multiple E-W to NE-SW trending lineaments and faults (Maurya, 1995).

The drainage network analysis reveals tectonic sensitivities of different watersheds. Because of tectonic adjustment along the major faults, regional slope of the valley and knickpoints have emerged. It is evident as major tectonic anomalies in the NE elevated zone of

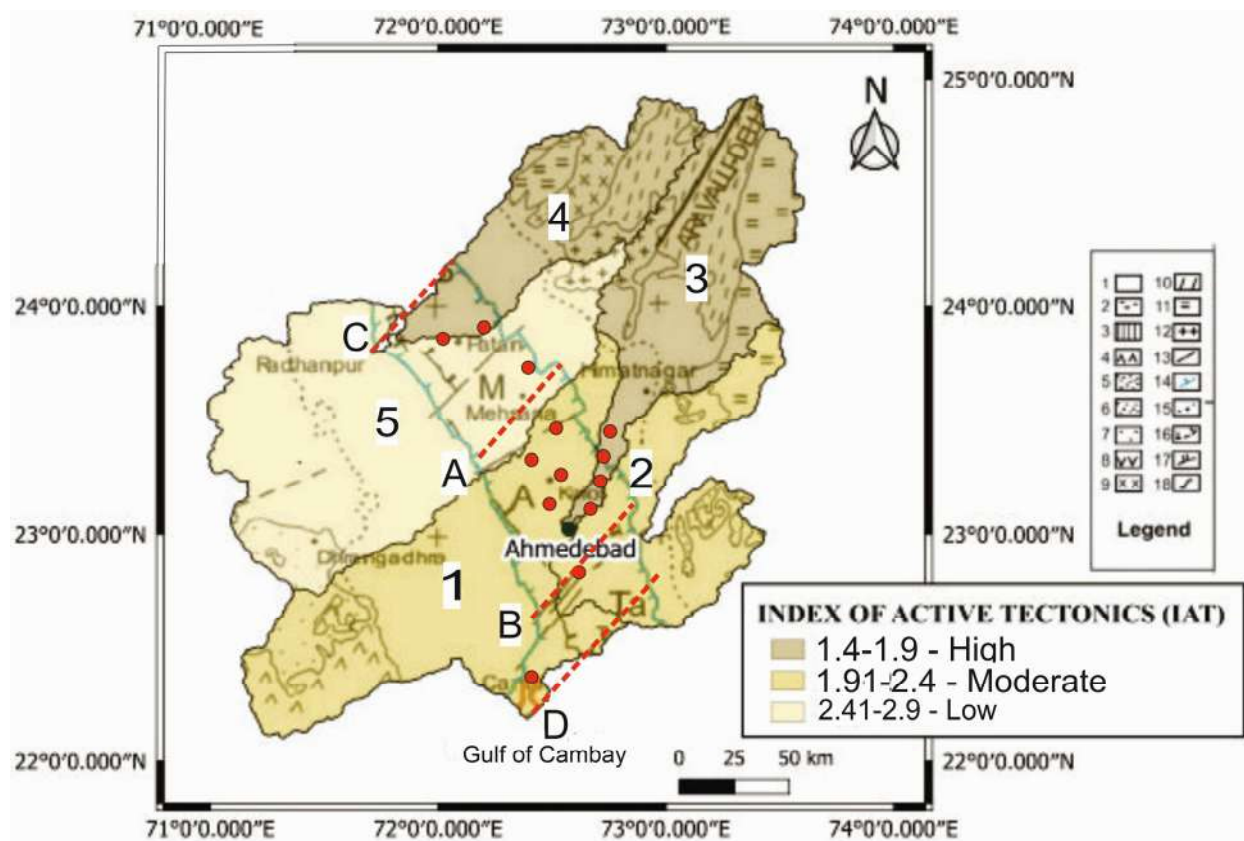


Fig. 4. Index of Active Tectonics map of the study area overlaid on the geologic map taken from Ganguli et al. (2018).. Watersheds 1, 5 and a part of 2 come under the alluvium. Watersheds 3 and 4 occur NW of the study area. The IAT map suggests that the NE area is more tectonically significant than the SW part. Hydrocarbon and tectonic blocks- A-B: Ahmedabad Mehsana, A-C: Patan Block, B-D: Tarapur Block. Red dots: oil fields. Major formations are (in background): 1. Alluvium, 2. Neogene sediments, 3. Paleogene sediments, 4. Deccan Trap, 5. Upper Cretaceous rocks, 6. Lower Cretaceous rocks, 7. Jurassic rocks, 8. Malani Igneous Suite, 9. Erinpura Granite, 10. Delhi Super Group, 11. Aravalli Super Group, 12. Archean Granite Gneiss, 13. Major Precambrian Trend, 14. Paleogene boundary of the Cambay Basin (rift margin), 15. Neogene boundary of the Cambay basin, 16. Primordial Fault, 17. Major Transfer Fault and 18. Coastline respectively. The oil field locations are plotted from Ganguli (2017) and Vishal et al. (2023)

Aravalli range where several prominent faults and lineaments in the NE part of CRB exist (watersheds 3 and 4) that ensure the stretch of area to be comparatively tectonically more active than the lower southern alluvial near the flat plains.

CONCLUSIONS

We investigated the tectonic geomorphology of the Cambay Rift Basin (CRB). The study reveals that watersheds 3 and 4 are tectonically more active than the watersheds 1, 2 and 5. The Precambrian Aravalli rocks, as well as some lineaments probably influenced recent tectonics of these two watersheds. The low-relief region termed as alluvial zone in the southern and westernmost part of the study area (portions of watersheds 1, 2 and 5), is comparatively less tectonically active. With the help of knick points, few tectonically active sites have been identified. The knickpoint analysis, together with SI and the IAT evaluation, reveal tectonic sensitivity in the NE portion within CRB in watershed 3. The geomorphic indices derived from the DEM of the region provide a strong input for studying neotectonics of CRB. The Ahmedabad-Mehsana block (part of watersheds 1, 3 and 4) in the middle part of CRB is also tectonically active and needs further studies for the well-bore stability issues since oil wells are located in that block. Cambay area has been studied for groundwater (e.g., Nikam et al., 2023), coal (Ojha and Singh 2023), coal-bed methane explorations (Ojha et al., 2023) and for hydrogen storage potential (Vishal et al., 2023). In these contexts also, the well-bore stability issue matters, and the present work stands relevant.

Acknowledgments: We thank the anonymous external reviewers, and the internal reviewers Dr. Swagato Dasgupta and Dr. Subhobroto Mazumder.

References

- Adhikary, P.P. and Dash, C.J. (2018) Morphometric Analysis of Katra Watershed of Eastern Ghats: A GIS Approach. *International Jour. Curr. Microbio. Appl. Sci.*, v.7, pp.1651-1665.
- Agarwal, R.P., Dotiwala, S., Mitra, D.S. and Bhoj, R. (1996) The palaeodelta of the "Proto" Vatrak and "Proto" Mahi rivers of northeastern Gujarat, India: A remote sensing interpretation. *Geomorphology*, v.15, pp.67-78.
- Alipoor, R., Poorkermani, M., Zare, M. and Hamdouni, R. E. (2011) Active tectonic assessment around Rudbar Lorestan dam site, High Zagros Belt (SW of Iran). *Geomorphology*, v.125, pp.1-14.
- Anand, A.K. and Pradhan, S.P. (2019) Assessment of active tectonics from geomorphic indices and morphometric parameters in part of Ganga basin. *Jour. Mount. Sci.*, v.16, pp.1943-1961.
- Aram, Z. and Arian, M. (2016) Active tectonics of the Gharasu river basin in Zagros, Iran, investigated by calculation of geomorphic indices and group decision using analytic hierarchy process (AHP) software. *Episodes*, v.39, pp.39-44.
- Argyriou, A.V., Teeuw, R.M., Rust, D. and Sarris, A. (2016) GIS multi-criteria decision analysis for assessment and mapping of neotectonic landscape deformation: a case study from Crete. *Geomorphology*, v.253, pp.262-274.
- Argyriou, A.V., Teeuw, R.M., Soupios, P. and Sarris, A. (2017) Neotectonic control on drainage systems: GIS-based geomorphometric and

- morphotectonic assessment for Crete, Greece. *Jour. Struct. Geol.*, v.104, pp.99-111.
- Babu, P.V.L.P. (1977) Geomorphology of the Cambay basin. *Jour. Indian Soc. Photo-Interpret.*, v.5(1), pp.9-17.
- Bahrami, S. (2012) Morphotectonic evolution of triangular facets and wine-glass valleys in the Noakoh anticline, Zagros, Iran: Implications for active tectonics. *Geomorphology*, v.159-160, pp.37-49.
- Baruah, M.P., Bezbaruah, D. and Goswami, T.K. (2020) Active tectonics deduced from geomorphic indices and its implication on economic development of water resources in South-Eastern part of Mikirmassif, Assam, India. *Geol., Ecol. Landscap.*, v.6, pp.99-112.
- Bierman, P.R. and Montgomery, D.R. (2014) Key concepts in geomorphology. WH Freeman.
- Birjandi, D., Derakhshani, R., Bafti, S.S. and Chatrouz, H. (2020) A morphotectonic survey on Golpayegan watershed using AHP method in GIS environment. *Sustainable Development of Mountain Territories*, v.12, pp.39-44.
- Biswas, M. and Paul, A. (2020) Application of geomorphic indices to Address the foreland Himalayan tectonics and landform deformation- Matiali-Chalsa-Baradighi recess, West Bengal, India. *Quaternary Internat.*, v.585, pp.1040-6182.
- Biswas, M., Paul, A. and Jamal, M. (2021) Tectonics and channel morpho-hydrology—a quantitative discussion based on secondary data and field Investigation. *In: S. Mukherjee (Ed.), Structural Geology and Tectonics Field Guidebook*. Springer, Vol.1, pp.461-494.
- Biswas, M., Puniya, M.K., Gogoi, M.P., Dasgupta, S., Mukherjee, S. and Kar, N.R. (2022) Morphotectonic analysis of petroliferous Barmer rift basin (Rajasthan, India). *Jour. Earth Syst. Sci.*, v.131, pp.140.
- Biswas, S. K. (2012) Status of petroleum exploration in India. *Proc. Natl. Acad. Sci., India*, v.78, pp.475-494.
- Biswas, S.K. (1982) Rift Basins in Western Margin of India and Their Hydrocarbon Prospects with Special Reference to Kutch Basin. *AAPG Bull.*, v.66, pp.1497-1513.
- Biswas, S.K. (1987) Regional tectonic framework, structure and evolution of the western marginal basins of India. *Tectonophysics*, v.135, pp.307-327.
- Biswas, S.K. (1999) A Review on the Evolution of Rift Basins in India During Gondwana with Special Reference to Western Indian Basins and Their Hydrocarbon Prospects. *Proc. Indian Natl. Sci. Acad. Spec. Iss.*, v.65, pp.261-283.
- Bull, W.B. and McFadden, L.D. (1977) Tectonic Geomorphology North and South of the Garlock Fault, California. *In: Doehring, D.O. (Ed.), Geomorphology in Arid Regions: A Proceedings Volume of the 8th Annual Geomorphology Symposium*, State University of New York, Binghamton, pp.115-138.
- Chen, Y.W., Shyu, J.B.H. and Chang, C.P. (2015) Neotectonic characteristics along the eastern flank of the Central Range in the active Taiwan orogen inferred from fluvial channel morphology, *Tectonics*, v.34, pp.2249-2270.
- Chen, Y.C., Sung, Q., Chen, C.N. and Jean, J.S. (2006) Variations in Tectonic Activities of the Central and Southwestern Foothills, Taiwan, Inferred from River Hack Profiles. *Terrestrial, Atmosph. Oceanic Sci.*, v.17, pp.563.
- Chorley, R.J. (1957) Illustrating the laws of morphometry. *Geol. Magz.*, v.94, pp.140-150.
- Choudhury, P., Chopra, S., Kamra, C. and Das, A. (2019) New Insight into the Recent Earthquake Activity in North Cambay Basin, Western India: Seismological and Geodetic Perspectives. *Bull. Seismol. Soc. Amer.*, v.109, pp.2240-2251.
- Chouhan, A. K., Choudhury, P. and Pal, S.K. (2023) Sedimentary Thickness and Upper Crustal Structure of the North Cambay Rift, India Deduced from Gravity Data: New Evidence of Pre-trappean Sediments. *Jour. Geol Soc India*, v.99(6), pp.773-782.
- Chouhan, A. K., Singh, D., Pal, S. K. and Choudhury, P. (2022) Delineation of subsurface geological fractures in the Cambay rift and surrounding regions of NW India: an integrated approach using satellite derived EIGEN-6C4 gravity data. *Geocarto Internat.*, v.37(1), pp.268-283.
- Clark, M.K., Schoenbohm, L.M., Royden, L.H., Whipple, K.X., Burchfiel, B.C., Zhang, X., Tang, W., Wang, E. and Chen, L. (2004) Surface uplift, tectonics, and erosion of eastern Tibet from large-scale drainage patterns. *Tectonics*, v.23, 1006.
- Clark, M.K., Schoenbohm, L.M., Royden, L.H., Whipple, K.X., Burchfiel, B. C. and Madan, M. (1995) Cambay Basin – A Promise of Oil and Gas Potential. *Jour. Palaeontol. Soc. India*, v.40, pp.41-47.
- Costigan, K. H., Daniels, M. D. and Perkin, J. S., Gido, K.B. (2014) Longitudinal variability in hydraulic geometry and substrate characteristics of a Great Plains sand-bed river. *Geomorphology*, v.210, 51.
- Cox, R.T. (1994). Analysis of drainage basin symmetry as a rapid technique to identify areas of possible Quaternary tilt-block tectonics: an example from the Mississippi Embayment. *Geol. Soc. Amer.*, v.106, pp.571-581.
- Danda, N., Rao, C.K. and Kumar, A. (2017) Geoelectric structure of northern Cambay rift basin from magnetotelluric data. *Earth Planets Space*, v.69, pp.140.
- Das, A. and Solanki, T. (2020) Geological Signatures of Tectonic Instability along the North Cambay Basin during the Late Holocene Period, North Gujarat, India. *Jour. Geol. Soc. India*, v.96, pp.584-590.
- Dasgupta, S. and Mukherjee, S. (2019) Remote sensing in lineament identification: Examples from western India. *In: Billi A, Fagereng A (Eds) Problems and Solutions in Structural Geology and Tectonics. Developments in Structural Geology and Tectonics Book Series. Vol. 5. Series Editor: Mukherjee S. Elsevier*, pp. 205-221.
- Dasgupta, S. and Mukherjee, S. (2017) Brittle shear tectonics in a narrow continental rift: asymmetric non-volcanic Barmer basin (Rajasthan, India). *Jour. Geol.*, v.125, pp561-591.
- Desai, N.P., Shukla, S.H. and Tandon, A. (2023) Exploring Geomorphic Features in Lower Sabarmati River Basin as Signatures of Palaeoenvironmental Change, Gujarat: A Remote Sensing Approach. *Jour. Geol. Soc. India*, v.99(2), pp.233-238.
- Dubey, R.K. and Shankar, R. (2019) Drainage Pattern and its Bearing on Relative Active Tectonics of a Region: A Study in the Son Valley, Central India. *Jour. Geol. Soc. India*, v.93, pp.693-703.
- Dwivedi, A. (2016) Petroleum Exploration in India - A perspective and Endeavours. *Proc. Natl. Acad. Sci., India*, v.82, pp.881-903.
- Elias, Z. (2015) The Neotectonic Activity Along the Lower Khazir River by Using SRTM Image and Geomorphic Indices. *Earth Sci.*, v.4-1, pp.2328-5982.
- Ganguli, S.S. (2017) Integrated reservoir studies for CO₂-enhanced oil recovery and sequestration: Application to an Indian mature oil field. Springer.
- Ganguli, S. S., Vedanti, N., Pandey, O. P., and Dimri, V. P. (2018) Deep thermal regime, temperature induced over-pressured zone and implications for hydrocarbon potential in the Ankleshwar oil field, Cambay basin, India. *Jour. Asian Earth Sci.*, v.161, pp.93-102
- Gentana, D., Sulaksana, N., Sukiyah, E. and Yuningsih, E.T. (2018) Index of Active Tectonic Assessment: Quantitative-based Geomorphometric and Morphotectonic Analysis at Way Belu Drainage Basin, Lampung Province, Indonesia. *Int. Jour. Adv. Sci. Infor. Tech.*, v.8, pp.2460-2471.
- Gupta, M.L. (1981) Surface heat flow and igneous intrusion in the Cambay basin India. *Jour. Volcanol. Geotherm. Res.*, v.10, pp.279-292.
- Gupta, S.D., Chatterjee, R., Farooqui, M.Y. (2012) Formation evaluation of fractured basement, Cambay Basin, India. *Jour. Geophys. Eng.*, v.9, pp.162-175.
- Gupta, S. and Biswas, M. (2022) Seismo-tectonic and morphological study of the north-east Himalaya. *Geosci. Jour.*, pp.1-21.
- Hack, J.T. (1957) Studies of Longitudinal Stream Profiles in Virginia and Maryland. USGS Prof. Paper, 294B, pp.45-97.
- Hack, J.T. (1973) Stream-profiles analysis and stream-gradient index. *Jour. Res. USGS*, v.1, pp.421-429.
- Hafiz, M. (2019) Source Potential and Reservoir Fabric of the Cambay Shale, Cambay Basin: A Potential Tight Gas/Tight Oil Resource for India. *Search and Discovery Article*, 11246
- Howard, A.D. (1967) Drainage analysis in geologic interpretation: a summation, *AAPG Bull.*, v.51, pp.2246- 2259.
- Kaila, K.L., Tewari, H.C., Krishna, V.G., Dixit, M.M., Sarkar, D. and Reddy, M.S. (1990) Deep seismic sounding studies in the north Cambay and Sanchar basins, India. *Geophys. Jour. Internat.*, v.103, pp.621-637.
- Keller, E.A. and Pinter, N. (2001) Active Tectonics, Earthquakes, Uplift, and Landscape, Earth Science Series, Prentice Hall, Englewood Cliffs, NJ.
- Khalid, L.A. and El-Ashmawy (2016) Investigation of The Accuracy of Google Earth Elevation Data. *Artificial Satellites*, v.51, 2016-0008.
- Kirby, E., and Whipple, K.X. (2012) Expression of active tectonics in erosional landscapes, *Jour. Struc. Geol.*, v.44, pp.54-75.
- Kumar, D., Singh, D.S. and Prajapati, S.K. (2018) Morphometric Parameters and Neotectonics of Kalyani River Basin, Ganga Plain: A Remote Sensing and GIS Approach. *Jour. Geol. Soc. India*, v.91, pp.679-686.
- Kumar, S. and Ojha, K. (2021) Reaction kinetic, maturity, burial and thermal

- histories modelling of Cambay shale source rocks, Cambay Basin, Western India. *Jour. Petrol. Sci. Eng.*, v.202, pp.108-543.
- Kumari, P., Kumari, R. and Kumar, D. (2021) Geospatial approach to evaluate the morphometry of Sabarmati River Basin, India. *Arab. Jour. Geosci.*, v.14, pp.206.
- Kundu, J., and Wani, M.R. (1992) Structural style and tectono-stratigraphic framework of Cambay rift basin, Western India. *Internat. Jour. Petrol. Geol.*, v.1, pp.181–202.
- Larue, J.P. (2008) Effects of tectonics and lithology on long profiles of 16 rivers of the southern Central Massif border between the Aude and the Orb (France). *Geomorphology*, v.93, pp.343–367.
- Larue, J.P. (2011) Longitudinal Profiles and Knick zones: The Example of the Rivers of the Cher Basin in the Northern French Massif Central. *Proc. Geologists' Assoc.*, v.122, pp.125-142.
- Leopold, L.B. and Maddock, T. (1953) The Hydraulic Geometry of Stream Channels and Some Physiographic Implications. *USGS Prof. Paper No. 252*, pp.1-57.
- Leopold, L.B., Wolman, M.G. and Miller, J.P. (1964) Fluvial processes in geomorphology, chapter 5, Drainage basin as a geometric unit. *WH Freeman and company, San Francisco and London.*
- Lu, P. and Shang, Y. (2015) Active Tectonics Revealed by River Profiles along the Puqu Fault. *Water*, v.7, pp.1628-1648.
- Magar, P.P. and Magar, N.P. (2016) Application of Hack's Stream Gradient Index (SL Index) to Longitudinal Profiles of the Rivers Flowing Across Satpura-Purna Plain, Western Vidarbha, Maharashtra. *Jour. Indian Geomorphology*, v.4, pp.64-72.
- Mahesh, P., Catherine, J.K., Gahalaut, V.K., Kundu, B., Ambikapathy, A., Bansal, A., Premkishore, L., Narsaiah, M., Ghavri, S., Chadha, R.K. and Choudhary, P. (2012) Rigid Indian plate: constraints from GPS measurements. *Gondwana Res.*, v.22, pp.1068-1072.
- Mahmood, S.A. and Gloaguen, R. (2012) Appraisal of active tectonics in Hindu Kush: Insights from DEM derived geomorphic indices and drainage analysis. *Geosci. Front.*, v.3, pp.407-428.
- Malik, J.N. and Mohanty, C. (2007) Active tectonic influence on the evolution of drainage and landscape: Geomorphic signatures from frontal and hinterland areas along the Northwestern Himalaya, India. *Jour. Asian Earth Sci.*, v.29, pp.604–618.
- Mathur, L.P., Rao, K.L.N. and Chaubey, A.N. (1968) Tectonic framework of Cambay basin, India. *Bull. ONGC*, v.5, pp.7–28.
- Maurya, D.M., Chamyal, L.S., Merh, S.S. (1995) Tectonic evolution of the Central Gujarat plain, Western India. *Curr. Sci.*, v.69, pp.610-613.
- Mazumder, S., Dave, H.D., Samal, J.K. and Mitra, D.S. (2012) Delineation of basement-related fault closures in eastern part of Purna basin based on morphotectonic analysis. *Assoc. Petrol. Geo. Bull.*, v.8, pp.41-47.
- Merh, S.S. and Chamyal, L.S. (1997) The Quaternary Geology of Gujarat Alluvial Plain, Indian National Science Academy, New Delhi, 98p.
- Mitra, D.S. and Agarwal, R.P. (1991) Geomorphology and petroleum prospects of cauvery basin, Tamilnadu, based on interpretation of Indian remote sensing satellite (IRS) data. *Jour. Indian Soc. Rem. Sens.*, v.19, pp.263-268.
- Mohan, K., Chaudhary, P., Kumar, G.P. and Rastogi, B.K. (2019) Magnetotelluric investigations in the southern end of the Cambay basin (near coast), Gujarat, India. *Jour. Appl. Geophys.*, v.162, pp.80–92.
- Mukherjee, S., Dole, G., Yatheesh, V. and Kale, V. (2020) Tectonics of the Deccan trap: Focus on Indian Geoscientists' Contribution in the Last Four Years. *In: Glimpse of Geoscience Researches in India. Proceedings of the Indian National Science Academy. Coordinators: D.M. Banerjee, S. Dasgupta, A.K. Jain, S. Bajpai*, v.86, pp.237-244.
- Mukherjee, S., Misra, A.A., Calvès, G. and Nemèok, M. (2017) Tectonics of the Deccan Large Igneous Province: an introduction. *In: Mukherjee S, Misra, A.A., Calvès, G, Nemèok, M. (Eds.), Tectonics of the Deccan Large Igneous Province. Geol. Soc. London, Spec. Publ.*, v.445, pp.1-9.
- Nagarjuna, D., Kumar, A., Pavankumar, G., Rao, C.K. and Manglik, A. (2023). Spatially heterogeneous lithospheric architecture of the Cambay rift basin and adjoining Aravalli-Delhi Fold Belt, western India—A synthesis of magnetotelluric results. *Tectonophysics*, v.861, 229905.
- Nikam, R., Pavankumar, G., Pancholi, V., Singh, D., Nagar, M., Nagarjuna, D. and Chopra, S. (2023) Geoelectrical study for groundwater resources in parts of the Ahmedabad and Gandhinagar cities, Gujarat, India. *Curr. Sci.*, v.124, pp.340.
- Ojha, S., Punjrath, N.K., Chakraborty, A. and Singh, P.K. (2023) Evolution and Evaluation of Coal-bed Methane in Cambay Basin, Western India: Insights from Stable Isotopic and Molecular Composition. *Jour. Geol. Soc. India*, v.99(2), pp.193-204.
- Ojha, S. and Singh, P.K. (2023) Petrogenesis and Evolution of Tharad Coals of Cambay Basin, Gujarat (Western India): An Insight. *Jour. Geol. Soc. India*, v.99(5), pp.675-687.
- Pancholi, V., Kothiyari, G.C., Prizomwala, S., Sukumaran, P., Shah, R.D., Bhatt, N.Y., Chauhan, M. and Kandregula, R.S. (2017) Morphotectonic of Sabarmati-Cambay basin, Gujarat, Western India. *Jour. Indian Geophys. Union*, v.21, pp.371-383.
- Pant, S., Kumar, A., Ram, M., Klochkov, Y. and Sharma, H.K. (2022) Consistency Indices in Analytic Hierarchy Process: A Review. *Mathematics*, v.10, 1206.
- Pande, C.B. and Moharir, K. (2015) GIS based quantitative morphometric analysis and its consequences: a case study from Shanur River Basin, Maharashtra India. *Appl. Water Sci.*, v.7, pp.861–871.
- Pati, J.K., Lal, J., Prakash, K. and Bhusan, R. (2008) Spatio-temporal shift of Western bank of the Ganga River, Allahabad City and its Implications. *Jour. Indian Soc. Rem. Sens.*, v.36, pp.289–297.
- Pati, J.K., Malviya, V.P. and Prakash, K. (2006) Basement re-activation and its relation to Neotectonic activity in and around Allahabad, Ganga Plain. *Jour. Indian Soc. Rem. Sens.*, v.34, pp.47–56.
- Phaye, D.K., Bhattacharya, B. and Chakrabarty, S. (2021) Heterogeneity characterization from sequence stratigraphic analysis of Paleocene-Early Eocene Cambay Shale formation in Jambusar-Broach area, Cambay Basin, India. *Marine Petrol. Geol.*, v.128, pp.104-986.
- Prakash, K., Mohanty, T., Pati, J.K., Singh, S. and Chaubey, K. (2017) Morphotectonics of the Jamini River basin, Bundelkhand Craton, Central India; using remote sensing and GIS technique. *Appl. Water Sci.*, v.7, pp.3767–3782.
- Ra'doane, M., Ra'doane, N. and Dumitriu, D. (2003) Geomorphological evolution of longitudinal river profiles in the Carpathians. *Geomorphology* v.50, pp.293–306.
- Raj, R. (2012) Active tectonics of NE Gujarat (India) by morphometric and morphostructural studies of Vatrak River basin. *Jour. Asian Earth Sci.*, v.50, pp.66–78.
- Raju, A.T.R. (1968) Geological Evolution of Assam and Cambay Tertiary Basins of India. *AAPG Bull*, v.52, pp.2422-2437.
- Rastogi, B.K., Kumar, S. and Aggrawal, S.K. (2013) Seismicity of Gujarat. *Natural Hazards*, v.65, pp.1027–1044.
- Saaty, T.L. (1980) *The Analytic Hierarchy Process*, McGraw-Hill, New York.
- Saaty, T. L. (1977) A scaling method for priorities in hierarchical structures. *Jour. Mathemat. Psychol.*, v.15, pp.234-281.
- Saaty, T.L. and Vargas, L.G. (1991) Prediction, projection and forecasting: applications of the analytic hierarchy process in economics, finance, politics, games and sports (pp. 11-31). Boston: Kluwer Academic Publishers.
- Saber, R., Isik, V. and Caglayan, A. (2020) Tectonic geomorphology of the Aras drainage basin (NW Iran): Implications for the recent activity of the Aras fault zone. *Geol. Jour.*, v.55, pp.5022– 5048.
- Sahoo, T.R. and Choudhuri, M. (2011) Tectono-Sedimentary Evolution of Northern part of Cambay Basin. The 2nd South Asian Geoscience Conference and Exhibition, GEOIndia.
- Shukla, S. (2013) Spatial Analysis of Drainage Network for Ground Water Exploration in River Basin using Gis and Remote Sensing Techni-ques: A Case Study of Tons River in Allahabad, India. *Jour. Environ. Res. Develop.*, v.7.
- Singh, C.K. (2014) Active deformations extracted from drainage geomorphology; a case study from Southern Sonbhadra district, Central India. *Jour. Geol. Soc. India*, v.84, pp.569–578.
- Singh, C.K. (2015) Middle Ganga plain; may be on the verge of seismic shock. *Jour. Geol. Soc. India*, v.85, pp.511–513.
- Sinha, S.K. and Parker, G. (1996) Causes of Concavity in Longitudinal Profiles of Rivers. *Water Resour. Res.*, v.32, pp.1417-1428.
- Sobel, E.H., Hilley, G.E. and Strecker, M. (2003) Formation of internally drained contractional basins by aridity-limited bedrock incision: *Jour. Geophys. Res.*, v.108, B7, 2.
- Sukristiyanti, S., Maria, R. and Lestiana, H. (2018) Watershed-based Morphometric Analysis: A Review. *IOP Conf. Series: Earth Environ. Sci.*, v.118, pp.012-028.

- Taesiria, V., Pourkermania, M., Sorbib, A., Almasiana, M. and Arianc, M. (2020) Morphotectonics of Alborz Province (Iran): A Case Study Using GIS Method. *Geotectonics*, v.54, pp.691–704.
- Troiani, F., Galve, J.P., Piacentini, D., Della, S.M., Guerrero, J. (2014) Spatial analysis of stream length-gradient (SL) index for detecting hillslope processes: A case of the Gállego River headwaters (Central Pyrenees, Spain). *Geomorphology*, v.214, pp.183–197.
- Verrios, S., Zygouri, V. and Kokkalas, S. (2004) Morphotectonic Analysis in The Eliki Fault Zone (Gulf of Corinth, Greece). *Bull. Geol. Soc. Greece*, v.36, pp.1706-1715.
- Vishal, V., Verma, Y., Sulekh, K., Singh, T.N. and Dutta, A. (2023) A first-order estimation of underground hydrogen storage potential in Indian sedimentary basins. Miocic, J. M., Heinemann, N., Edlmann, K., Alcalde, J. and Schultz, R. A. (eds) *Enabling Secure Subsurface Storage in Future Energy Systems*. Geol. Soc. London, Spec. Publ., v.528(1), SP528-2022.
- Wani, M.R. and Kundu, J. (1995) Tectonostratigraphic analysis in Cambay rift basin: Leads for future exploration. *In: Proc. First Internat. Petrol. Conf. B. R. Publishing Corporation Delhi*. pp.147-174.
- Whipple, K.X., Di-Biase, R.A., Crosby, B.T. (2013) *Bedrock Rivers, Treatise on Geomorphology*, v.9, pp.550-570.
- Whipple, K.X. and Tucker, G.E. (1999) Dynamics of the stream-power river incision model: Implications for height limits of mountain ranges, landscape response timescales, and research needs. *Jour. Geophys. Res.*, v.104, pp.17661-17674.
- Withjack, Martha., Schlische, Roy. and Olsen, Paul. (2002) Rift-basin structure and its influence on sedimentary systems. *In: Sedimentation in Continental Rifts*, v.73, pp.57–81.
- Wobus, C.W., Crosby, B.T. and Whipple, K.X. (2005) Hanging valleys in fluvial systems: Controls on occurrence and implications for landscape evolution. *Jour. Geophys. Res. Earth Surf.*, v.111, F02017.
- Wobus, C.W., Whipple, K.X., Kirby, E., Snyder, N., Johnson, J., Spyropolou, K., Crosby, B. and Sheehan, D. (2006) Tectonics from topography: Procedures, promise, and pitfalls. *Spec. Paper Geol. Soc. Amer.*, no.398, pp55–74.
- Wolosiewicz, B. (2018) The influence of the deep-seated geological structures on the landscape morphology of the Dunajec River catchment area, Central Carpathians, Poland and Slovakia. *Contemporary Trends of Geoscience*, v.7, pp.21-47.
- Wood, L., Sanyal, S., Dwivedi, N. and Burlet, D.S. (2010) A Subsurface Taj Mahal: Seismic Geomorphology Calibrated with Core and Log Data Provides Key Building Blocks for Modeling Tidally-Influenced Estuarine Deposits in the Gulf of Cambay, Western India. *In: Seismic Imaging of Depositional and Geomorphic Systems: 30th Annual*, pp.210-211.
- Zaprowski, B.J., Pazzaglia, F.J. and Evenson, E.B. (2005) Climatic influences on profile concavity and river incision. *Jour. Geophys. Res.*, v.110, 0148-0227.
- Zernitz, E.R. (1932) Drainage patterns and their significance. *Jour. Geol.*, v.40, pp.498–521.
- Zhang, X., Tang, W., Wang, E., Chen, L. (2004) Surface uplift, tectonics, and erosion of eastern Tibet from large-scale drainage patterns. *Tectonics*, v.23, TC1006.
- Zhenkui, G., Changxing, S., Jie, P. (2019) Evolutionary dynamics of the main-stem longitudinal profiles of ten kongdui basins within Inner Mongolia, Chinese Geograph. Sci., v.29, pp.417-431.
- Zovoili, E., Konstantinidi, E., Koukouvelas, I.K. (2004) Tectonic geomorphology of escarpments: the cases of Kompotades and Nea Anchialos faults. *Bull. Geol. Soc. Greece*, v.36, pp.1716–1725.



Surabhi, K.N., did B.Sc. and M.Sc. in Geology in 2019 and 2021, respectively. Specialization: morphometry.



Mery Biswas studied Geography and received Bachelors and Masters degrees in 2000 and 2002, respectively. Specialization: morphometry, NE Himalayan tectonics.



Soumyajit Mukherjee did B.Sc., M.Tech. and Ph.D. in Applied) Geology in 1999, 2002 and 2007, respectively. Teaches structural geology and stratigraphy.